The Canadian Mineralogist
Vol. 36, pp. 1045-1051 (1998)

SYNTHESIS AND RIETVELD REFINEMENT OF NEW PHOSPHATE AND ARSENATE ANALOGUES OF PARACELSIAN

FRANÇOIS LUCAS[1], AMMY ELFAKIR, GILLES WALLEZ AND MICHEL QUARTON

Laboratoire de Cristallochimie du Solide, Université Pierre et Marie Curie, 4, place Jussieu,
F-75252 Paris Cedex 05, France

MARTINE LAGACHE

Laboratoire de Géologie, Ecole Normale Supérieure, 24, rue Lhomond, F-75005 Paris, France

ABSTRACT

Two new arsenates with the general formula $A^{2+}(ZnAsO_4)_2$ (A = Sr, Ba) were synthesized by solid-state reaction. Furthermore, $Ba(ZnPO_4)_2$ was obtained under hydrothermal conditions. X-ray diffractograms of these compounds were indexed with a monoclinic unit-cell, and their structures were refined by the Rietveld method using reported atomic coordinates for paracelsian $Ba(AlSiO_4)_2$. Comparison of these structures with those of aluminosilicate and gallogermanate isomorphs illustrates a strong deviation to the pseudo-orthorhombic symmetry that may be explained by the very different charges and ionic radii of the tetrahedrally coordinated cations. Distortions of the tetrahedral sites as well as of the network of tetrahedra are found. The paracelsian form of $Ba(ZnPO_4)_2$ may only be obtained under hydrothermal conditions and at a high temperature (T = 500°C, P = 2 kbar); it undergoes an irreversible transition at T = 800°C and ambient pressure to a hexagonal form with space group $P\bar{3}m1$.

Keywords: paracelsian, monoarsenate, monophosphate, Rietveld analysis, polymorphism.

SOMMAIRE

Nous avons synthétisé par réaction à l'état solide deux nouveaux arséniates $A^{2+}(ZnAsO_4)_2$ (A = Sr, Ba) et, sous conditions hydrothermales, le phosphate $Ba(ZnPO_4)_2$. Les trois composés ont été indexés dans le système monoclinique et leur structure a été affinée par la méthode de Rietveld sur le modèle du paracelsian $Ba(AlSiO_4)_2$. La comparaison de ces structures avec celles des aluminosilicates et de leurs isomorphes gallogermanates met en évidence un grand écart à la symétrie pseudo-orthorhombique. Cet écart s'explique essentiellement par les grandes différences de taille et de charge entre les cations à coordinence tétraédrique. Cette distorsion est présente tant au niveau des tétraèdres d'oxygène que du squelette tridimensionnel construit à partir de ces derniers. La forme paracelsian de $Ba(ZnPO_4)_2$ n'a pu être obtenue que sous une pression de 2 kbars et à une température de 500°C; elle présente à pression ambiante (T = 800°C) une transition irréversible vers une forme hexagonale de groupe d'espace $P\bar{3}m1$.

Mots-clés: paracelsian, monoarséniate, monophosphate, analyse de Rietveld, polymorphisme.

INTRODUCTION

We have recently reported the crystal structures, phase transitions and dielectric properties of some of $A^+T^{2+}PO_4$ monophosphates and their arsenate counterparts (Jaulmes *et al.* 1993, Wallez *et al.* 1995). We have extended our investigations to $A^{2+}T^{2+}{}_2X^{5+}{}_2O_8$ compounds, where A represents strontium or barium, T, magnesium or zinc, and X, phosphorus or arsenic. These compounds are of particular structural interest because their framework is sufficiently flexible to allow phase transitions, their constituent elements are in their highest oxidation state, and the presence of two different tetrahedrally coordinated cations is liable to suppress the centrosymmetry for ferroelectric properties. Furthermore, the study of these phases is interesting in view of their complex polymorphism (Malcherek *et al.* 1995) and their relationships with the extensive family of feldspar-type structures, especially those with formula $A^{2+}Al_2Si_2O_8$ (Smith 1953, Newnham & Megaw 1960, Kempster *et al.* 1962, Takéuchi *et al.* 1973, Kroll & Phillips 1976, Griffen *et al.* 1977) and their synthetic gallogermanates analogues (Dal Negro *et al.* 1978, Gazzoni 1973, Phillips *et al.* 1975, Calleri & Gazzoni 1976).

---

[1] *E-mail address*: flucas@ccr.jussieu.fr

$A^{2+}B_2P_2O_8$ compounds have been widely synthesized and characterized (Sarver *et al.* 1961, Hoffman 1965, Bakakin *et al.* 1975, Jakerman & Cheetham 1988, Hemon & Courbion 1990, El Bali *et al.* 1993), but no information has been published on their behavior under high pressure or on their homologous arsenates. In the present paper, we report the synthesis and powder-diffraction refinement of the structure of a high-pressure phosphate, $BaZn_2P_2O_8$, and two new arsenates, $SrZn_2As_2O_8$ and $BaZn_2As_2O_8$, with the structure of paracelsian.

SYNTHESIS AND CHARACTERIZATION

The synthesis of the compounds was carried out by high-temperature sintering of stoichiometric amounts of MCO_3 (M: Sr, Ba), ZnO (first dried at 700°C), $NH_4H_2PO_4$ or As_2O_5; xH_2O (a hygroscopic compound; x determined to be 3/5 by Thermal Gravimetry Analysis). The powder mixtures were thoroughly mixed, placed in a platinum crucible, and heated to 400°C (with loss of H_2O, NH_3, CO_2). They were then reground and fired at 900°C for 72 hours with intermediate remixing. Finally, the samples were slowly cooled to room temperature.

For the phosphate compound, the microcrystalline powder obtained by solid-state reaction was used as starting material for hydrothermal growth. Water was added in suitable volume to give a 70% filling ratio in a gold tube that was sealed and enclosed in a steel vessel. The vessel was kept at 500°C for three weeks in a vertical tube furnace. The calculated vapor pressure in the capsule at these conditions is 2000 bars.

TABLE 1. CRYSTALLOGRAPHIC DATA AND CHARACTERISTICS OF REFINEMENT, STRUCTURAL ANALOGUES OF PARACELSIAN

Data collection

Diffractometer	17 cm vertical diffractometer (Philips PW 1050/25)
Instrument power	40 kV, 20 mA
Radiation	Cu$K\bar{\alpha}$, λ = 1.54178 Å
Discrimination	Ni filter in diffracted beam
Detector	Proportional counter (Xe)
Stepsize (2θ)	0.02°
Steptime (cumulated)	15 s
Divergence angle	1°
Width, receiving slit	0.1 mm
Soller slits	Two sets (in incoming and diffracted beams)
Temperature	20°C
Geometry, data collection	Bragg – Brentano parafocussing θ – 2θ
2θ limits	$12 < 2\theta < 82°$
Ranges of indices collected	$0 \le h \le 7, 0 \le k \le 8, -7 \le l \le 7$

Crystallographic data

	$Ba(ZnPO_4)_2$	$Ba(ZnAsO_4)_2$	$Sr(ZnAsO_4)_2$
Crystal system	Monoclinic	Monoclinic	Monoclinic
Space group	$P2_1/c$ (#14)	$P2_1/c$ (#14)	$P2_1/c$ (#14)
Cell parameters			
a (Å)	8.5783(1)	8.8083(2)	8.5804(2)
b (Å)	9.7383(1)	9.9821(3)	9.7183(3)
c (Å)	9.1446(1)	9.4089(3)	9.2908(2)
β (°)	91.394(1)	91.465(1)	92.085(1)
V (Å^3) (Z = 4)	763.69(4)	827.00(4)	774.22(4)
Formula weight (g.mol^{-1})	458.02	545.92	496.20
Observed reflections	459	502	499
Final agreement-factors (%)			
R_p	5.19	3.74	4.01
R_{wp}	6.65	5.29	5.35
R_B	6.28	3.69	3.90
R_F	3.36	2.49	3.09

An automated vertical Philips powder diffractometer was used to record the diffraction patterns of the three materials. The powder patterns were indexed on the basis of a monoclinic unit-cell using the automatic indexing program TREOR (Werner 1985). Unit-cell parameters were then refined using the least-squares method (Table 1).

STRUCTURE REFINEMENT

On the basis of their X-ray diffractograms and the indexed peaks, these compounds seem to be isostructural with the paracelsian form of $Ba(AlSiO_4)_2$. The structure refinement was thus initiated using reported atomic coordinates for paracelsian (Chiari *et al.* 1985). Zinc was assigned to the aluminum site and phosphorus or arsenic takes the place of silicon.

TABLE 2. FRACTIONAL ATOMIC COORDINATES AND THERMAL PARAMETERS, $Ba(ZnPO_4)_2$, $Ba(ZnAsO_4)_2$ AND $Sr(ZnAsO_4)_2$

Atom	x	y	z	B_{iso} (Å^2)
Ba	0.2518(2)	0.4164(2)	0.8970(2)	0.35(6)
T_1o (Zn)	0.9270(3)	0.9271(3)	0.2089(3)	0.34(6)
T_1m (P)	0.5549(7)	0.9110(6)	0.2420(6)	0.34(6)
T_2o (P)	0.9564(7)	0.2050(6)	0.0677(6)	0.34(6)
T_2m (Zn)	0.5831(4)	0.1810(3)	0.0588(3)	0.34(6)
O_1o	0.998(1)	0.1143(8)	0.195(1)	0.9(1)
O_1m	0.491(1)	0.0500(9)	0.194(1)	0.9(1)
O_2o	0.945(1)	0.3488(9)	0.125(1)	0.9(1)
O_2m	0.545(1)	0.362(1)	0.136(1)	0.9(1)
O_3o	0.086(1)	0.196(1)	0.959(1)	0.9(1)
O_3m	0.447(1)	0.190(1)	0.8828(9)	0.9(1)
O_4	0.8005(8)	0.168(1)	0.007(1)	0.9(1)
O_5	0.7221(8)	0.912(1)	0.2991(9)	0.9(1)
Ba	0.2500(2)	0.4147(2)	0.8908(2)	0.90(6)
T_1o (Zn)	0.9286(3)	0.9250(3)	0.2207(3)	0.40(4)
T_1m (As)	0.5593(3)	0.9119(3)	0.2451(2)	0.40(4)
T_2o (As)	0.9472(3)	0.2022(3)	0.0653(3)	0.40(4)
T_2m (Zn)	0.5791(4)	0.1854(3)	0.0535(3)	0.40(4)
O_1o	0.005(1)	0.1081(8)	0.199(1)	1.7(1)
O_1m	0.499(1)	0.0598(9)	0.190(1)	1.7(1)
O_2o	0.939(1)	0.3585(8)	0.122(1)	1.7(1)
O_2m	0.558(1)	0.3640(9)	0.132(1)	1.7(1)
O_3o	0.080(1)	0.190(1)	0.9481(9)	1.7(1)
O_3m	0.444(1)	0.195(1)	0.8862(9)	1.7(1)
O_4	0.7856(8)	0.148(1)	0.001(1)	1.7(1)
O_5	0.7313(8)	0.924(1)	0.3144(9)	1.7(1)
Sr	0.2525(2)	0.4161(2)	0.8872(2)	1.03(7)
T_1o (Zn)	0.9285(3)	0.9285(3)	0.2209(3)	0.70(5)
T_1m (As)	0.5586(3)	0.9152(3)	0.2513(2)	0.70(5)
T_2o (As)	0.9518(3)	0.2043(3)	0.0606(3)	0.70(5)
T_2m (Zn)	0.5789(3)	0.1851(3)	0.0490(3)	0.70(5)
O_1o	0.026(1)	0.1115(8)	0.196(1)	1.4(1)
O_1m	0.487(1)	0.0625(8)	0.190(1)	1.4(1)
O_2o	0.935(1)	0.3672(8)	0.117(1)	1.4(1)
O_2m	0.561(1)	0.3728(9)	0.122(1)	1.4(1)
O_3o	0.082(1)	0.203(1)	0.9394(8)	1.4(1)
O_3m	0.432(1)	0.199(1)	0.8794(8)	1.4(1)
O_4	0.7878(8)	0.141(1)	0.002(1)	1.4(1)
O_5	0.7330(8)	0.940(1)	0.3291(9)	1.4(1)

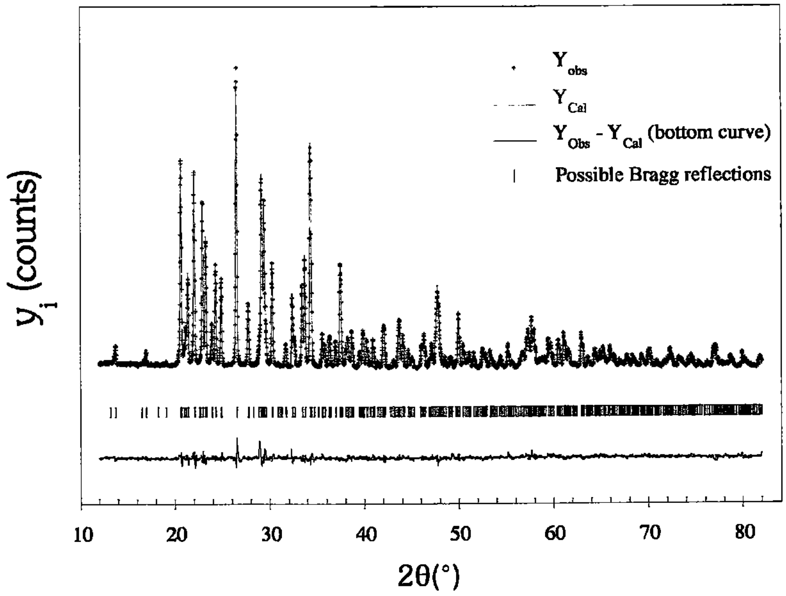

FIG. 1. The observed, calculated and difference patterns for $Sr(ZnAsO_4)_2$.

The refinement was performed using the FULLPROF program (Rodriguez-Carjaval 1995), a modification of the code DBW3.2 (Wiles & Young 1981). Peak-profile refinement included a pseudo-Voigt function and an asymmetry correction for small angles ($2\theta < 40°$). The background was described using a five-parameter polynomial function. Scattering curves for neutral atoms were taken from the International Tables for X-ray Crystallography (1995).

Refinement of the 58 independent parameters (both instrumental and structural) resulted in convergence at the end of each refinement. Final agreement factors are listed in Table 1. Atomic positions are given in Table 2, and Figure 1 illustrates, as an example, the agreement between observed and calculated patterns of $SrZn_2As_2O_8$.

DESCRIPTION OF THE STRUCTURE

Except for minor shifts in atomic positions (Table 2), the three compounds are isostructural with their aluminosilicate and gallogermanate counterparts. Zinc, phosphorus and arsenic are totally ordered in the tetrahedra. Each ZnO_4 tetrahedron shares its oxygen atoms with four PO_4 or AsO_4 and *vice versa*. The resulting structure may be described as a (100) pseudolayered framework of 4- and 8-membered rings (Fig. 2). Two groups of atoms may therefore be defined: those with an x coordinate close to 0 (o plane) and those with an x coordinate close to ½ (m plane). The o and m planes are related by a pseudomirror at $x \approx$ ¼. The connection between sheets along the **a** axis occurs by 4- and 6-membered rings roughly parallel to (011) and (0$\bar{1}$1) planes by means of the two remaining apical oxygen atoms, O_4 and O_5 (Fig. 3). The large Ba or Sr atoms occupy cavities between layers. They adopt a 7-fold coordination illustrated by a monocapped octahedron. The O_{1o}, O_{2m}, O_{3o}, O_{3m} and O_5 atoms are approximately

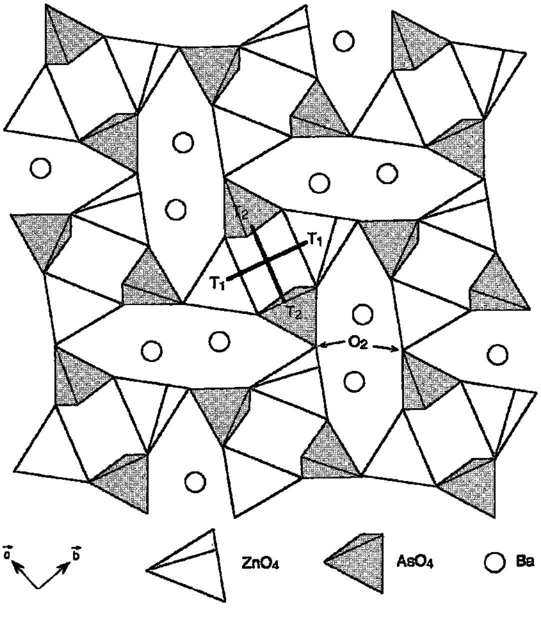

FIG. 2. The 4- and 8-member rings of tetrahedra in the *m* pseudolayer.

TABLE 3. INTERATOMIC DISTANCES AND ANGLES, $BaZn_2(PO_4)_2$, $BaZn_2(AsO_4)_2$ AND $SrZn_2(AsO_4)_2$

T - O Distances (Å)

	BaZnP*	BaZnAs*	SrZnAs*
T_1o-O_1o	1.93(1)	1.962(9)	1.980(9)
-O_2o	2.00(1)	1.98(1)	1.968(9)
-O_3o	1.94(1)	1.96(1)	1.961(9)
-O_5	1.964(8)	1.970(8)	1.990(8)
Mean	1.96	1.97	1.975
T_1m-O_1m	1.52(1)	1.648(9)	1.651(9)
-O_2m	1.50(1)	1.64(1)	1.64(1)
-O_3m	1.50(1)	1.63(1)	1.648(9)
-O_5	1.513(9)	1.638(8)	1.656(8)
Mean	1.51	1.64	1.65
T_2o-O_1o	1.50(1)	1.639(9)	1.657(9)
-O_2o	1.50(1)	1.652(9)	1.674(9)
-O_3o	1.51(1)	1.631(9)	1.613(9)
-O_4	1.48(1)	1.625(1)	1.612(8)
Mean	1.50	1.637	1.639
T_2m-O_1m	1.96(1)	1.94(1)	1.95(1)
-O_2m	1.94(1)	1.94(1)	1.953(9)
-O_3m	1.96(1)	1.953(9)	1.985(9)
-O_4	1.936(8)	1.934(8)	1.909(8)
Mean	1.95	1.94	1.95

O - O distances (Å) and O - T - O angles (°)

	BaZnP*	BaZnAs*	SrZnAs*	BaZnP*	BaZnAs*	SrZnAs*
O_1o-O_2o	3.10(1)	3.04(1)	2.95(1)	104.0(9)	101.1(7)	96.9(7)
-O_3o	3.40(1)	3.36(1)	3.42(1)	123(1)	118(1)	120(1)
-O_5	3.23(1)	3.25(1)	3.29(1)	113(1)	111.4(8)	111.9(8)
O_2o-O_3o	3.28(1)	3.32(1)	3.28(1)	112(1)	114.8(9)	113.2(9)
-O_5	2.99(1)	3.02(1)	2.96(1)	97.7(7)	100.0(7)	96.8(6)
O_3o-O_5	3.09(1)	3.22(1)	3.31(1)	104.5(8)	110.1(8)	113.9(8)
O_1m-O_2m	2.43(1)	2.63(1)	2.59(1)	107(1)	106(1)	103.5(9)
-O_3m	2.50(1)	2.69(1)	2.72(1)	111(1)	111(1)	111(1)
-O_5	2.56(1)	2.70(1)	2.71(1)	114(1)	111(1)	110.0(9)
O_2m-O_3m	2.48(1)	2.68(1)	2.76(1)	111(1)	110(1)	114(1)
-O_5	2.43(1)	2.67(1)	2.66(1)	108(1)	109(1)	107.4(9)
O_3m-O_5	2.40(1)	2.68(1)	2.72(1)	105(1)	110(1)	111(1)
O_1o-O_2o	2.41(1)	2.66(1)	2.70(1)	107(1)	108.0(9)	108.2(9)
-O_3o	2.44(1)	2.60(1)	2.61(1)	108(1)	105.1(9)	105.7(9)
-O_4	2.44(1)	2.68(1)	2.69(1)	110(1)	110(1)	111(1)
O_2o-O_3o	2.47(1)	2.68(1)	2.65(1)	110(1)	109(1)	107.2(9)
-O_4	2.40(1)	2.73(1)	2.73(1)	107(1)	113(1)	112(1)
O_3o-O_4	2.51(1)	2.68(1)	2.68(1)	114(1)	111(1)	112.1(9)
O_1m-O_2m	3.12(1)	3.13(1)	3.15(1)	106.6(9)	107.5(8)	107.4(8)
-O_3m	3.17(1)	3.19(1)	3.19(1)	107.8(9)	109.9(9)	108.3(8)
-O_4	3.39(1)	3.25(1)	3.26(1)	121(1)	113.7(9)	114.9(9)
O_2m-O_3m	2.97(1)	3.02(1)	2.99(1)	99.3(8)	101.5(8)	98.9(7)
-O_4	3.14(1)	3.22(1)	3.20(1)	108.6(9)	112.2(9)	112.1(8)
O_3m-O_4	3.22(1)	3.21(1)	3.27(1)	111.4(9)	111.4(8)	113.9(8)

T - O - T angles (°)

	BaZnP*	BaZnAs*	SrZnAs*
O_1o	122(1)	120.8(8)	115.2(7)
O_1m	128(1)	132(1)	127.3(9)
O_2o	126(1)	121.8(8)	118.0(7)
O_2m	132(1)	127.2(9)	122.8(8)
O_3o	122(1)	125.4(9)	121.5(8)
O_3m	126(1)	125.3(9)	119.6(7)
O_4	140(1)	131.4(9)	130.6(8)
O_5	135(1)	129.7(8)	122.4(7)
Mean	129	127	122

A - O distances (Å) (A = Sr, Ba)

	BaZnP*	BaZnAs*	SrZnAs*
A-O_1o	2.84(1)	2.79(1)	2.60(1)
O_1m	2.82(1)	2.94(1)	2.78(1)
O_2o	2.85(1)	2.808(9)	2.650(9)
O_2m	2.80(1)	2.79(1)	2.607(9)
O_3o	2.65(1)	2.76(1)	2.59(1)
O_3m	2.78(1)	2.78(1)	2.62(1)
O_5	2.79(1)	2.774(9)	2.644(9)
Mean	2.79	2.81	2.64

*BaZnP for $BaZn_2(PO_4)_2$, BaZnAs for $BaZn_2(AsO_4)_2$, SrZnAs for $SrZn_2(AsO_4)_2$

located at five vertices of a slightly irregular octahedron, whereas $O1_m$ and $O2_o$ complete the polyhedron at much greater *M*–O distances. In Table 3, we report the values of interatomic distances and angles for the three compounds $BaZn_2P_2O_8$, $BaZn_2As_2O_8$ and $SrZn_2As_2O_8$, denoted BaZnP, BaZnAs and SrZnAs, respectively.

DISTORTION OF THE TETRAHEDRA

To compare the refined structures with other analogues of paracelsian, we used the σ_{tet} parameter previously defined by Baur (1974):

$$\sigma_{tet} = \sum_{i=1}^{6} \frac{\left|(O-T-O)_i - \langle O-T-O \rangle_m\right|}{6\langle O-T-O \rangle_m} \times 100$$

where $(O-T-O)_i$ is the individual angle for a given tetrahedron, and $\langle O-T-O \rangle_m$ is the average angle for a regular tetrahedron (*e.g.*, 109.47°). Calculated values of s are given in Table 4.

Distortion of the tetrahedra arises from two factors: a) T_1 and T_2 tetrahedra are not structurally equivalent. Each T_2 tetrahedron has three corners in common with the alkaline-earth polyhedra, whereas the T_1 tetrahedron shares one edge and two corners. As a result, T_1 sites

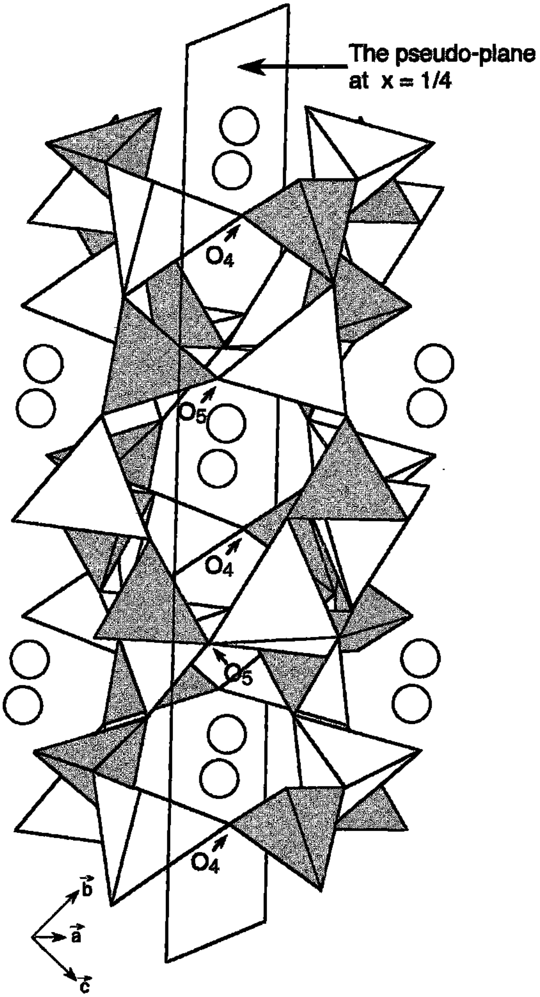

FIG. 3. Perpective view of the connection between *o* and *m* pseudolayers.

TABLE 4. TETRAHEDRON-DISTORSION PARAMETERS IN PARACELSIAN AND ITS STRUCTURAL ANALOGUES

	BaAlSi	SrGaSi	SrGaGe	BaGaGe	BaZnP	BaZnAs	SrZnAs
σ_{T1O} (Al, Ga or Zn)	3.86	5.06	5.60	5.06	6.36	5.22	7.06
σ_{T1m} (Si, Ge or P, As)	2.80	3.32	4.51	4.58	2.44	1.22	2.46
σ_{T2O} (Si, Ge or P, As)	1.53	1.61	2.06	2.14	1.83	1.81	2.13
σ_{T2m} (Al, Ga or Zn)	2.11	2.79	2.63	2.71	4.42	2.93	4.00
$\sigma_{(Si, Ge or P,As)}$ / $\sigma_{(Al, Ga or Zn)}$	0.76	0.63	0.80	0.86	0.40	0.37	0.42
σ_{T2}/σ_{T1}	0.55	0.53	0.46	0.50	0.71	0.74	0.64

Sources of data: $BaAl_2Si_2O_8$: Chiari *et al.* (1985), $SrGa_2Si_2O_8$ and $SrGa_2Ge_2O_8$: Phillips *et al.* (1975), $BaGa_2Ge_2O_8$: Calleri & Gazzoni (1976).

are more distorted than the chemically identical T_2 sites, and the σ_{T2}/σ_{T1} ratio is therefore less than 1 (Table 4). b) The charge and ionic radius of the tetrahedrally coordinated cations are likely to strongly influence the degree of distortion. The higher the charge and the smaller the radius, the more the tetrahedrally coordinated cation becomes polarized in its anionic environment; furthermore, as bond strength increases, the distortion decreases. The importance of size and charge can be evaluated from the ratio of $\sigma(T^{4(5)+})$ to $\sigma(T^{3(2)+})$ (Table 4).

The results (Tables 3, 4) highlight the relative importance of factors described above for each compound: 1) For analogues of paracelsian in which tetrahedrally coordinated cations show a small difference in size and charge (silicates and germanates), the distortion is mainly controlled by the structural environment of the tetrahedra; physical factors intervene also, but to a lesser extent, as deduced from the high value of the $\sigma(T^{4(5)+})/\sigma(T^{3(2)+})$ parameter.

2) For the phosphate and arsenate compounds, the four T^{5+}–O bond lengths are very regular, as are the bond angles. The bond lengths are more irregular, and the distortion parameters, greater, for zinc–oxygen tetrahedra, whatever their connectivity.

FRAMEWORK DISTORTION AND BOND LENGTHS

With the aim of examining the distortions of the three-dimensional framework as a function of the radii of the cations, Calleri & Gazzoni (1976) defined an empirical degree of ellipticity $(T_1–T_1)/(T_2–T_2)$ for each of the four *o* and *m* rings belonging to one layer (Fig. 2). Analysis of these values of ellipticity (Table 5) highlights how the framework adapts itself to the size of the tetrahedrally coordinated cation. The isomorphs of paracelsian show a degree of ellipticity nearly identical in *o* and *m* rings. However, because of the large difference in size between zinc and arsenic or phosphorus cations, a non-uniform variation in the degree of ellipticity of the four-membered rings is observed for the two kinds of layers in these compounds. Owing to

TABLE 5. THE (T1–T1) OR (T2–T2) DEGREE OF ELLIPTICITY OF TYPE-o AND TYPE-m FOUR-MEMBERED RINGS IN PARACELSIAN AND ITS STRUCTURAL ANALOGUES

	BaAlSi	SrGaSi	SrGaGe	BaGaGe	BaZnP	BaZnAs	SrZnAs
Type o	1.094	1.110	1.150	1.127	1.009	1.062	1.077
Type m	1.126	1.202	1.193	1.152	1.224	1.232	1.274

Sources of data: $BaAl_2Si_2O_8$: Chiari *et al.* (1985), $SrGa_2Si_2O_8$ and $SrGa_2Ge_2O_8$: Phillips *et al.* (1975), $BaGa_2Ge_2O_8$: Calleri & Gazzoni (1976).

the presence of the large Zn^{2+} ion at the extremities of the T_1–T_1 major segment, the distances between crystallographically equivalent cations T_1–T_1 and T_2–T_2 are similar for the *o* layers. On the other hand, if the smaller As or P cations lie on this axis (in the *m* layer), a strong distortion of the rings results, as well as a significant increase of the corresponding ellipticity.

Analysis of (*T*–O–*T*) angles for oxygen atoms belonging to pseudolayers is very instructive. In paracelsian, the values seem quite similar. On the contrary, for the arsenates and the phosphate, the (*T*–O–*T*) values depend very much on whether atoms belong to the *o* or the *m* layer. For oxygen atoms of the *m* layer, corresponding angles are always larger than for oxygen atoms of the *o* layer, with the exception of O_{3o}; this findng may be explained by the abnormally short distance of this atom from the central cation (Table 3).

In conclusion, consideration of the degree of ellipticity and (*T*–O–*T*) angles highlights the differences in framework between the paracelsian analogues and the new compounds reported here. The former are characterized by similarities between *o* and *m* layers and a slight deviation from the pseudo-orthorhombic structure. The latter are relatively highly distorted, as a result of the adaptation of the flexible framework of tetrahedra to the very different charges and sizes of the two tetrahedrally coordinated cations. The distortion is not uniform throughout the structure; the *o* layer collapses around the Sr or Ba atoms, as seen in the smaller (*T*–O–*T*) angles and the very weak ellipticity of the four-membered rings; the *m* layer presents larger angles, greater ellipticity, and consequently a larger distortion of the paracelsian structure.

PHASE TRANSITION

The two arsenates exhibit nearly identical melting points, approximately 1060–1070°C. Furthermore, a slight dip of the Differential Thermal Analysis signal in the vicinity of the melting reaction (1020°C) is observed. High-temperature X-ray-diffraction analysis confirms the existence of an allotropic form with a high degree of symmetry, which may be isotypic with the hexagonal form of celsian (Takéuchi 1958), but the proximity to the melting point and the difficulty in distinguishing neighboring thermal signals at such a temperature did not allow a satisfactory characterization.

The case of $Ba(ZnPO_4)_2$ seems very different; the paracelsian form was only obtained under hydrothermal conditions. The crystal form resulting from heating the initial mixture under atmospheric pressure is trigonal (*a* 5.31, *c* 8.02 Å), with space group $P\bar{3}m1$, and may be related to the hexagonal form of celsian by introducing complete Zn–P order among the tetrahedra (in prep.). The change from one allotropic form to the other may be achieved either by pressure or temperature modification in agreement with the following scheme:

$$\begin{array}{c}\text{Hexagonal}\\\text{form}\end{array}\;\underset{\begin{array}{c}\text{2 kbar}\\T = 500^\circ\text{C in water}\end{array}}{\overset{\begin{array}{c}\text{1 bar}\\T_c = 800^\circ\text{C}\end{array}}{\leftrightarrows}}\;\begin{array}{c}\text{Paracelsian}\\\text{form}\end{array}$$

REFERENCES

Bakakin, V. , Rylov, G. & Alekseev, V. (1975): Refinement of the crystal structure of horlbathite $CaBe_2P_2O_8$. *Sov. Phys. Crystallogr.* **19**, 798-803.

Baur, H.W. (1974): The geometry of polyhedral distortions. Predictive relationships for the phosphate group. *Acta Crystallogr.* **B30**, 1195-1215.

Calleri, M. & Gazzoni, G. (1976): The structures of $(Sr,Ba)[(Al,Ga)_2(Si,Ge)_2O_8]$. III. The crystal structures of paracelsian-like modifications of synthetic $SrGa_2Ge_2O_8$ and $BaGa_2Ge_2O_8$. *Acta Crystallogr.* **B32**, 1196-1205.

Chiari, G., Gazzoni, G., Craig, J.R., Gibbs, G.V. & Louisnathan, S.J. (1985): Two independent refinement of the structure of paracelsian, $BaAl_2Si_2O_8$. *Am. Mineral.* **70**, 969-974.

Dal Negro, A., De Pieri, R. & Quareni, S. (1978): The crystal structures of nine K-feldspars from the Adamello massif (northern Italy). *Acta Crystallogr.* **B34**, 2699-2707.

El Bali, B., Boukhari, A., Aride, J. & Abraham, F. (1993): The crystal structure of $SrNi_2(PO_4)_2$. *J. Solid State Chem.* **104**, 453-459.

Gazzoni, G. (1973): Al–Ga and Si–Ge diadochy in synthetic $BaAl_2Si_2O_8$ and $SrAl_2Si_2O_8$. *Z. Kristallogr.* **137**, 24-34.

Griffen, D.T., Ribbe, P.H. & Gibbs, G.V. (1977): The structure of slawsonite, a strontium analogue of paracelsian. *Am. Mineral.* **62**, 31-35.

Hemon, A. & Courbion, G. (1990): The crystal structure of α-$SrZn_2(PO_4)_2$: a hurlbutite type. *J. Solid State Chem.* **85**, 164-168.

Hoffman, M.V. (1965): The systems BaO–MgO–P_2O_5 and BaO–ZnO–P_2O_5. Compounds and fluorescence. *J. Electrochem. Soc.* **110**, 1223-1227.

International Tables for X-Ray Crystallography (1995): Vol. C. Kluwer, Dordrecht, The Netherlands (477-499).

Jakerman, R.J.B. & Cheetham, A.K. (1988): Combined single-crystal X-ray diffraction and magic angle spinning NMR study of α-$CaZn_2(PO_4)_2$. *J. Am. Chem. Soc.* **110**, 1140-1143.

Jaulmes, S., Wallez, G., Elfakir, A. & Quarton, M. (1993): Crystal and structure determination of the monoarsenate CsBeAsO4. *Eur. J. Solid State Inorg. Chem.* **30**, 1007-1015.

KEMPSTER, C.J.E., MEGAW, H.D. & RADOSLOVICH, E.W. (1962): The structure of anorthite $CaAl_2Si_2O_8$. I. Structure analysis. *Acta Crystallogr.* **15**, 1005-1035.

KROLL, H. & PHILLIPS, M.W. (1976): Comparison of feldspar and paracelsian-type structures. *Z. Kristallogr.* **143**, 285-299.

MALCHEREK, T., KROLL, H, SCHLEITER, M. & SALJE, E.K.H. (1995): The kinetics of the monoclinic to monoclinic phase transitions in $BaAl_2Ge_2O_8$-feldspar. *Phase Transitions* **55**, 199-215.

NEWNHAM, R.E. & MEGAW, H.D. (1960): The crystal structure of celsian (barium feldspar). *Acta Crystallogr.* **13**, 303-313.

PHILLIPS, M.W., KROLL, H. & PENTINGHAUS, H. (1975): The structures of synthetic paracelsian analogues, $SrGa_2Si_2O_6$ and $SrGa_2Ge_2O_8$. *Am. Mineral.* **60**, 659-666.

RODRIGUEZ-CARJAVAL, J. (1995): FULLPROF: Rietveld, profile matching and integrated intensity refinement of X-ray and/or neutron data (version 3.1.c). Laboratoire Léon Brillouin, CEA, Saclay, France.

SARVER, J.F., HOFFMAN, M.V. & HUMMEL, F.A. (1961): Phase equilibria and tin-activated luminescence in strontium orthophosphate systems. *J. Electrochem. Soc.* **108**, 1103-1110.

SMITH, J.V. (1953): The crystal structure of paracelsian, $BaAl_2Si_2O_8$. *Acta Crystallogr.* **6**, 613-620.

TAKÉUCHI, Y. (1958): A detailed investigation of the structure of hexagonal $BaAl_2Si_2O_8$ with reference to its $\alpha-\beta$ inversion. *Mineral. J.* **2**, 311-332.

________, HAGA, N. & ITO, J. (1973): The crystal structure of monoclinic $CaAl_2Si_2O_8$: a case of monoclinic structure closely simulating orthorhombic symmetry. *Z. Kristallogr.* **137**, 380-398.

WALLEZ, G., JAULMES, S., ELFAKIR, A. & QUARTON, M. (1995): Stereochemical activity of thallium (I) lone pair in the tridymite-related compounds $TlBePO_4$ and $TlBeAsO_4$. *J. Solid State Chem.* **114**, 123-128.

WERNER, P., ERICSSON, L. & WESTDAHL, M. (1985): TREOR, a semi-exhaustive trial and error powder indexing program for all symmetries. *J. Appl. Crystallogr.* **24**, 987-993.

WILES, D. & YOUNG, R. (1981): A new computer program for Rietveld analysis of X-ray powder diffraction patterns. *J. Appl. Crystallogr.* **14**, 149-151.

Received December 17, 1997, revised manuscript accepted May 22, 1998.